Observations of Collision-Induced Dipole Transitions Associated with High-Lying States of Calcium in Rare Gases

AUTHOR(S):

UEDA, Kiyoshi; ASHIZAWA, Yasuo; FUKUDA, Kuniya

Observations of Collision-Induced Dipole Transitions Associated with High-Lying States of Calcium in Rare Gases

By

Kiyoshi UEDA*, Yasuo ASHIZAWA,* and Kuniya FUKUDA*

(Received March 29, 1980)

Abstract

More than 20 collision-induced dipole (CID) transitions have been observed in the absorption spectrum of calcium below 2400 A in the presence of xenon or krypton. Some have also been observed in the presence of argon, neon or helium. The measured shifts and the effective oscillator strengths show a close correlation with the s-wave amplitude for the electron scattering by a rare-gas atom. This correlation leads us to the conclusion that the low-energy-electron-scattering process is responsible for the appearance of the CID transitions.

1. Introduction

It has been noted by many observers that weak collision-induced dipole (CID) transitions appear in the absorption (or emission) spectra of the alkali metals in rare-gas atmospheres. For example, CID transitions of cesium were observed by Lapp,[1] Gwinn *et al.*,[2] Dakhil and Kielkopf,[3] Happer and coworkers[4,5] etc.

Theoretical investigations were also made for these CID transitions. Gallagher and Holstein[6] explained quantitatively the red-side absorption band for $6s$-$5d$ of cesium in xenon[5] by the successive application of the quadrupole-dipole interaction (collisional perturbation) and radiative perturbation. Pascale[7] calculated the absorption oscillator strengths for the CID transitions on the basis of the adiabatic mixing of alkali-atom states. Recent experiments by Sayer *et al.*[8,9] showed a reasonable agreement with this calculation. However, these theories are concerned with CID transitions between the ground state and the lowest excited D or S state of alkali atoms. A quantitative explanation has never been given for CID transitions associated with the high-lying states reported in

* Department of Engineering Science

refs. 1–3.

Recently, we reported the observations of CID transitions associated with high-lying states of barium[10,11] and calcium[12] in rare-gas atmospheres. These observations have shown a correlation between CID transitions and low-energy-electron-scattering parameters. The correlation is qualitatively explained by a simple model introduced in ref. 11. This model assumes that a CID transition of this type arises from a mixing of closely-lying P states into the S, D, F,...upper states of the transition, due to the interaction of the loosely-bound electron with the rare-gas atom.

The model based on the electron-rare gas interaction has so far never been introduced with regard to an explanation of the CID transition. However, this model has been successfully applied to explain various phenomena related to the collisions of Rydberg atoms. For example, Fermi[13] explained the spectral shifts of alkali-atom lines[14] from this viewpoint for the first time. Recently, a similar approach has been applied by Hickman[15] and by Matsuzawa[16] to explain l-changing collisions of Rydberg atoms.[17–20]

Both the intrinsic interest in CID transitions and the improvement of our experimental technique have led us to re-examine and extend our previous observations of calcium.[12] The objective of this work is to determine whether any correlation exists between CID transitions and low-energy-electron-scattering parameters. In previous observations, we found a correlation between the effective oscillator strengths for CID transitions and low-energy-electron-scattering cross sections of rare-gas atoms. It is also of interest to examine whether the shifts of CID transitions have any correlation with the low-energy-electron-scattering parameters.

The general experimental arrangement and procedures are described in §2. Details of the results are given in §3. The observed correlation between CID transitions and low-energy-electron-scattering parameters is summarized in §4 with some discussions.

2. Experiment

An absorption method has been applied to observe CID transitions of calcium (below 2400 Å) in rare-gas atomspheres. The general experimental arrangement is shown in Fig. 1. This is almost the same as that described in ref. 11, but some improvements are given.

Calcium vapor was contained in a heat-pipe cell heated over the central 60 cm length to 1120–1290°K. We admixed rare gas of 80–960 mb in the cells as

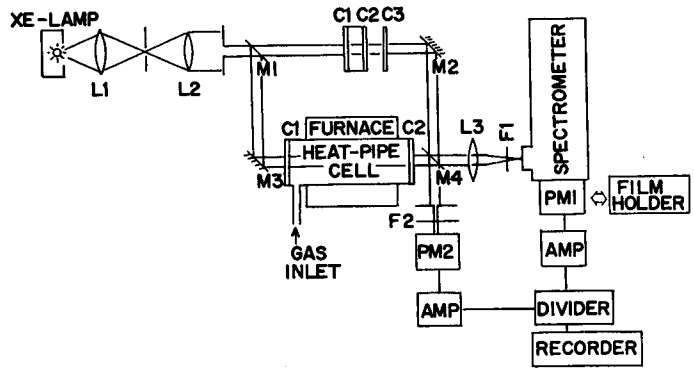

Fig. 1. General experimental arrangement: L1-L2, lenses; M1-M4, mirrors; F1 and F2, filters; C1-C3, quartz windows or plates.

the perturber. The cell temperature was monitored with platinum vs platinum-rhodium thermocouple, and it was kept within ± 1 degree with a SCR thermo-controller during the measurement of over several hours. The rare-gas density was determined from the cell temperature, and the gas pressure was measured by a diaphragm pressure gauge.

A xenon-arc lamp was used as a continuum light source, and spectra were observed with a 170 cm Ebert-mounting spectrometer. A grating having 1200 grooves/mm and blazed at 3000 Å was used in the first order, giving the reciprocal linear dispersion of 4.7 Å/mm in the wavelength region concerned.

By applying the hook method to the resonance line of calcium (λ 4227 Å) with the absorption oscillator strength 1.75,[21] the product of the calcium density [Ca] and the absorption length L was determined. In Fig. 1 four mirrors form the Mach-Zehnder interferometer. The absorption cell was placed in the test-beam section of the interferometer. For each condition of the density and the temperature, hook spectra were recorded on Kodak Tri-X film immediately before and after the absorption measurement. By this procedure it was ensured that the calcium density was kept constant during the absorption measurement. The change was 1 % typically and 3 % in the worst case. The typical value of $[Ca]L$ was 3×10^{18} cm^{-2} at 1280°K.

Photo-electric absorption measurements were carried out by the following procedure. In Fig. 1, the light path of the reference beam section of the interferometer was masked, and the transmitted light through the cell was observed by a spectrometer equipped with an EMI 6256B photomultiplier (PM1). The slit width used was typically 50 μm, resulting in an instrumental width of 0.25 Å. In order to compensate for the intensity fluctuation of the light source with time, the

output signal from PM1 was divided by the reference signal from PM2, as shown in Fig. 1. As the wavelength selection for PM2, a narrowband filter centered at 2537 Å was employed. The output signal from the divider was recorded by a strip chart recorder. These measurements were carried out under several conditions of temperatures and rare-gas pressures. To minimize the statistical error, the wavelength scan was repeated 2–10 times for each condition. During the scan, light from an iron- or a cupper-hollow-cathod lamp was admitted into the entrance slit to give the wavelength reference.

Under the conditions of $[X] \simeq 5 \times 10^{18}$ cm^{-3} and $[Ca]L \simeq 3 \times 10^{18}$ cm^{-2} at 1280°K, the absorption spectra below 2400 Å were recorded on Kodak SWR film together with the emission lines from the iron- and cupper-hollow-cathod lamps as the wavelength reference. The slit width was 30 μm, resulting in an instrumental width of 0.15 Å. The exposure times were 20 sec—3 min. for the absorption spectrum and 10 min. for the reference emission spectrum.

3. Results

3.1. Absorption spectra

More than 20 CID transitions were observed in the absorption spectra of calcium in the presence of xenon or krypton. Some examples of the spectra observed by the photo-electric method are shown in Fig. 2 (a)-(e), where xenon gas of 320 mb was used as the perturbing gas. The limited resolution of our spectrometer prevented us from measuring the detailed absorption profiles. Instead, we measured the total absorption

$$A = \int_{\text{band}} \{[1-\exp(-k(\nu)L]\}\mathrm{d}\nu \qquad (1)$$

for each of the CID transitions with the absorption coefficient $k(\nu)$. Figure 3 shows examples of the results by open points. As in the previous case of barium[10,11], the measured total absorption increases linearly with an increase of [Xe] as well as of [Ca]. Saturation occurs at large absorption. This linear dependence allows us to distinguish the CID transition from other atomic lines or Ca_2 bands.

We measured the peak wavelengths of most of the CID transitions and the impurity lines, employing the emission lines of Fe I and/or Cu I as references. This was done either on the microdensitometer traces of the spectrograms on the SWR films or on the chart traces of the photo-electric observations. In both cases, most of the measurements fit into a standard deviation better than 0.15 Å. For some CID transitions, we measured the peak wavelengths on the chart traces employing the impurity lines as references. In this case, the location was ac-

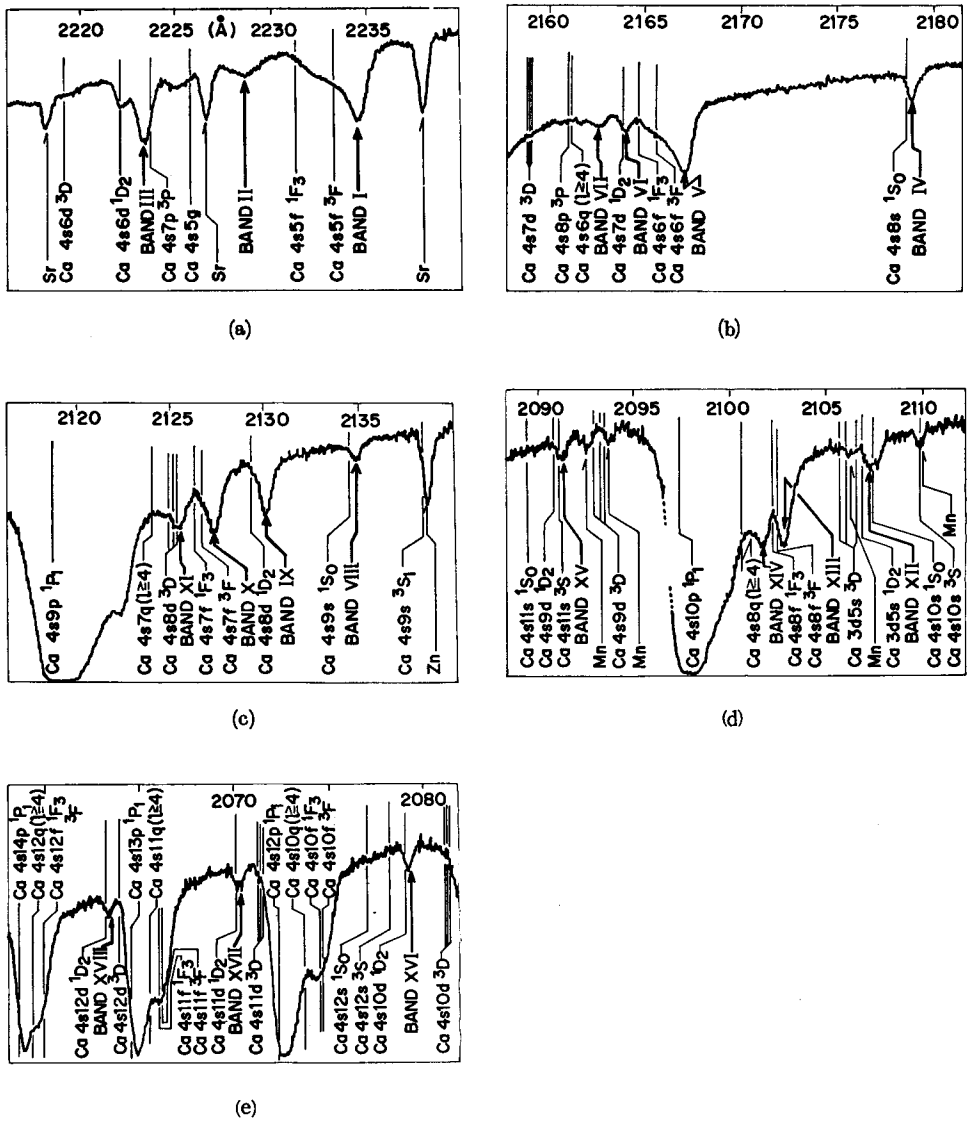

Fig. 2. Absorption spectra for the CID transitions: (a) Bands I, II and III; (b) Bands IV, V, VI, and VII; (c) Bands VIII, IX, X and XI; (d) Bands XII, XIII, XIV and XV; (d) Bands XVI, XVII and XVIII. The cell temperature is 1290°K, and [Xe] and [Ca]L are 1.8×10^{18} cm^{-3} and 3.0×10^{18} cm^{-2}, respectively. Wavelengths of the unperturbed atomic transitions are indicated by bars. For the manifold states of $l\geq4$, the quantum defects are assumed to be 0. (See §3.2 in text.) The absorption lines of impurity Sr, Zn and Mn are also indicated by thin arrows.

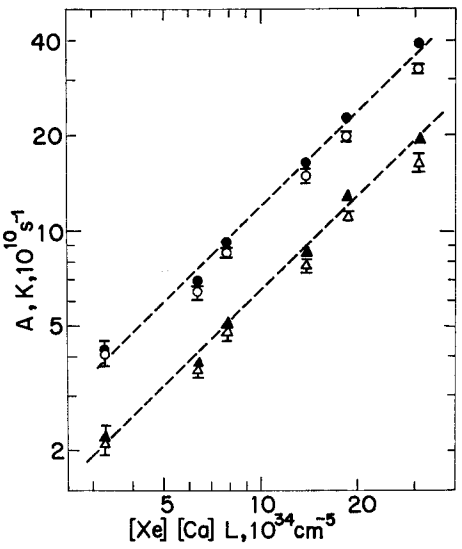

Fig. 3. Total absorption A in frequency units for the CID transitions: ○, $4s^2\,{}^1S_0-4p^2\,{}^1S_0$; △, $-4s7s\,{}^1S_0$. The closed points ▲ and ● refer to the K values with corrections for the opacity effect. The dashed lines with a slope of unity give the results of the weighted fit to the closed points. (See § 3.4 in text.)

Table I. Observed CID transitions from $4s^2\,{}^1S_0$ in Ca-Xe system.

Observed		Upper levels		
(A)	(cm^{-1})			(cm^{-1})
2393.02±0.13	41775.5±2.3	$4p^2$	$^1S_0$	41786.28[b]
2362.26±0.17*	42319.4±3.1	$4s4f$	$^1F_3$	42343.59[b]
2332.03±0.14*	42867.9±2.6	$4s5d$	$^1D_2$	42919.07[a]
2258.55±0.11	44262.5±2.2	$4s7s$	$^1S_0$	44276.54[a]
I)2234.36±0.15	44741.6±3.0	$4s5f$	$^1F_3$?	44804.88[b]
II)2228.56±0.15*	44858.1±3.0	$4s5g$	?	44916.23[c]
III)2223.11±0.15	44968.0±3.0	$4s6d$	$^1D_2$	44989.88[a]
IV)2179.04±0.15	45877.4±3.2	$4s8s$	$^1S_0$	45887.20[a]
V)2167.15±0.10	46129.1±2.1	$4s6f$	$^1F_3$?	46182.40[b]
VI)2164.01±0.15*	46196.0±3.3	$4s7d$	$^1D_2$?	46199.23[a]
VII)2162.63±0.16*	46225.4±3.4	$4s6q$	($l\geqq4$) ?	46257.46[c]
VIII)2134.71±0.10	46830.0±2.2	$4s9s$	$^1S_0$	46835.05[a]
IX)2129.95±0.13	46934.6±2.9	$4s8d$	$^1D_2$	46948.98[a]
X)2127.15±0.11	46996.4±2.4	$4s7f$	$^1F_3$?	47015.14[b]
XI)2125.38±0.16*	47035.5±3.5	$4s7q$	($l\geqq4$) ?	47066.18[c]
XII)2107.34±0.17*	47438.2±3.8	$3d5s$	$^1D_2$	47449.36[a]
XIII)2102.74±0.13	47541.9±2.9	$4s8f$	$^1F_3$?	47555.23[b]
XIV)2101.49±0.19*	47570.2±4.3	$4s8q$	($l\geqq4$) ?	47591.07[c]
XV)2091.10±0.10	47806.5±2.3	$4s9d$	$^1D_2$	47812.57[a]
XVI)2079.18±0.11	48080.6±2.5	$4s10d$	$^1D_2$	48083.42[a]
XVII)2070.25±0.12	48287.9±2.8	$4s11d$	$^1D_2$	48291.01[a]
XVIII)2063.44±0.14	48447.3±3.3	$4s12d$	$^1D_2$	48451.73[a]
2058.23±0.14	48569.9±3.3	$4s13d$	$^1D_2$	48578.40[a]

a) See ref. 23. b) See ref. 22.
c) Quantum defect is assumed to be 0. See § 3.2 in text.
I-XVIII) Bands I-XVIII. See Fig. 2 (a)-(e).
* Impurity lines (Sr, Zn) are employed as wavelength references.

Table II. Observed CID transitions from $4s^2\ {}^1S_0$ in Ca-Kr system.

Observed		Upper levels		
(A)	(cm^{-1})			(cm^{-1})
2392.79±0.12	41779.5±2.1	$4p^2$	$^1S_0$	41786.28[b]
2361.74±0.25*	42328.7±4.5	$4s4f$	$^1F_3$	42343.59[b]
2358.18±0.26*	42393.5±4.7	$4s4f$	$^1F_3$	42343.59[b]
2330.68±0.10	42892.8±1.8	$4s5d$	$^1D_2$	42919.07[a]
2258.24±0.09	44268.6±1.8	$4s7s$	$^1S_0$	44276.54[a]
2232.58±0.12	44777.3±2.4	$4s5f$	$^1F_3$?	44804.88[b]
2228.32±0.18*	44862.9±3.7	$4s5g$	?	44916.23[c]
2222.64±0.13	44977.5±2.6	$4s6d$	$^1D_2$	44989.88[a]
2178.62±0.16	45886.2±3.4	$4s8s$	$^1S_0$	45887.20[a]
2165.68±0.09	46160.4±1.9	$4s6f$	$^1F_3$?	46182.40[b]
2163.84±0.18*	46199.6±3.8	$4s7d$	$^1D_2$?	46199.23[a]
2162.49±0.16*	46228.5±3.4	$4s6q$	($l \geqq 4$) ?	46257.46[c]
2134.67±0.09	46830.9±2.0	$4s9s$	$^1S_0$	46835.05[a]
2129.59±0.09	46942.6±2.0	$4s8d$	$^1D_2$	46948.98[a]
2126.75±0.10	47005.3±2.2	$4s7f$	$^1F_3$?	47015.14[b]
2125.15±0.16*	47040.4±3.5	$4s7q$	($l \geqq 4$) ?	47066.18[c]
2107.06±0.17*	47444.5±3.8	$3d5s$	$^1D_2$	47449.36[a]
2102.53±0.09	47546.7±2.0	$4s8f$	$^1F_3$?	47555.23[b]
2101.43±0.16*	47571.5±3.6	$4s8q$	($l \geqq 4$) ?	47591.07[c]
2091.04±0.11	47807.9±2.5	$4s9d$	$^1D_2$	47812.57[a]
2079.20±0.11	48080.1±2.5	$4s10d$	$^1D_2$	48083.42[a]
2070.26±0.11	48287.7±2.6	$4s11d$	$^1D_2$	48291.01[a]
2063.42±0.10	48447.7±2.4	$4s12d$	$^1D_2$	48451.73[a]
2058.09±0.11	48573.2±2.6	$4s13d$	$^1D_2$	48578.40[a]

[a] See ref. 23. [b] See ref. 22.
[c] Quantum defect is assumed to be 0. See § 3.2 in text.
* Impurity lines (Sr, Zn) are employed as wavelength references.

Table III. Observed CID transitions from $4s^2\ {}^1S_0$ in Ca-Ar system.

Observed		Upper levels		
(A)	(cm^{-1})			(cm^{-1})
2392.82±0.11	41779.0±1.9	$4p^2$	$^1S_0$	41786.28[b]
2257.99±0.09	44273.5±1.8	$4s7s$	$^1S_0$	44276.54[a]
2231.47±0.25*	44799.6±5.0	$4s5f$	$^1F_3$?	44804.88[b]
2164.66±0.15	46182.1±3.2	$4s6f$	$^1F_3$?	46182.40[b]
2129.36±0.25*	46947.6±5.5	$4s8d$	$^1D_2$	46948.98[a]

[a] See ref. 23. [b] See ref. 22.
* Impurity lines (Sr, Zn) are employed as wavelength references.

curate to 0.15–0.26 Å. Tables I and II show the measured wavelengths and corresponding wavenumbers of the CID transitions of calcium due to xenon and krypton, respectively.

Some of these transitions are also observed in argon, neon, or helium. The measured wavelengths and the corresponding wavenumbers are given in Tables III, IV, and V.

Table IV. Observed CID transitions from $4s^2\ ^1S_0$ in Ca-Ne system.

Observed		Upper levels	
(A)	(cm^{-1})		(cm^{-1})
2327.74±0.15*	42946.9±2.8	$4s5d\ ^1D_2$	42919.07[a]
2257.61±0.15*	44280.9±2.9	$4s7s\ ^1S_0$	44276.54[a]

[a] See ref. 23.
* Impurity lines of Sr are employed as wavelength references.

Table V. Observed CIDtransitions from $4s^2\ ^1S_0$ in Ca-He system.

Observed		Upper levels	
(A)	(cm^{-1})		(cm^{-1})
2392.24±0.16	41789.1±2.8	$4p^2\ ^1S_0$	41786.28[b]
2325.37±0.25*	42990.7±4.6	$4s5d\ ^1D_2$	42919.07[a]
2257.42±0.20*	44284.6±3.9	$4s7s\ ^1S_0$	44276.54[a]
2192.12±0.15*	46952.9±3.3	$4s8d\ ^1D_2$	46948.98[a]

[a] See ref. 23. [b] See ref. 22.
* Impurity lines (Sr, Zn) are employed as wavelength references.

3.2. Assignments

Table I-V include "tentative" assignments of the upper levels of the transitions.[22,23] Our assignments are based on two assumptions. 1) The observed CID transitions have no selection rule for the orbital angular momentum of L or l. As for the selection rule for the spin S, however, $\Delta S=0$ is assumed to be valid for the S-S, S-D, and S-F transitions. 2) Since we have no information on the location of the "manifold" states of $l\geq 4$, we assume the quantum defects of these levels to be 0 for predicting the positions of the unperturbed atomic transitions (see Fig. 2).

On the basis of these assumptions, *e.g.*, in Fig. 2(a), Band I which extends towards the red from the position of the atomic transition $4s^2\ ^1S_0$-$4s5f\ ^1F_3$ is assigned to the CID transition to $4s5f\ ^1F_3$, which is abbreviated below by $-4s5f\ ^1F_3$. Band II is assigned to $-4s5g$, and Band III lying close to the small absorption line of the atomic electric-quadrupole transition $4s^2\ ^1S_0$-$4s6d\ ^1D_2$ is assigned, not to $-4s7p\ ^3P$,

but to -$4s6d\ ^1D_2$.

In Fig. 2(b), Band VI, the total sbsorption of which has an approximate linear dependence on [Xe], is assigned to -$4s7d\ ^1D_2$. In the presence of argon or neon, we observed a weak absorption line, or a band, the total absorption of which depends weakly on [Ar] or [Ne] at almost the same position as that of Band VI in Xe. Thus, Band VI is considered to include a small atomic electric-quadrupole transition line.

Band XII in Fig. 2(d) is assigned to -$3d5s\ ^1D_2$, but this includes a small band to $4s10s\ ^1S_0$.

3.3. The shift

The energy difference between the observed position of the CID transition and the predicted position of the unperturbed transition is called "shift". Table VI shows the shifts for the CID transitions in all rare gases. Some general features

Table VI. The shifts (cm^{-1}) of the CID transitions from $4s^2\ ^1S_0$.

Upper levels		Xe	Kr	Ar	Ne	He
$4p^2$	$^1S_0$	−10.8±2.3	− 6.8±2.1	− 7.3±1.9	—	+ 2.8±2.8
$4s4f$	$^1F_3$	−24.2±3.1	−14.9±4.5	—	—	—
$4s4f$	$^1F_3$	—	+49.9±4.7	—	—	—
$4s5d$	$^1D_2$	−51.1±2.6	−26.3±1.8	—	+27.9±2.8	+71.6±4.6
$4s7s$	$^1S_0$	−14.1±2.2	− 8.0±1.8	− 3.1±1.8	+ 4.4±2.9	+ 8.1±3.9
$4s5f$	$^1F_3$?	−63.2±3.0	−27.6±2.4	− 5.3±5.0	—	—
*$4s5g$	?	−58.1±3.0	−53.3±3.7	—	—	—
$4s6d$	$^1D_2$	−21.8±3.0	−12.3±2.6	—	—	—
$4s8s$	$^1S_0$	− 9.8±3.2	− 1.0±3.4	—	—	—
$4s6f$	$^1F_3$?	−53.3±2.1	−22.0±1.9	− 0.3±3.2	—	—
$4s7d$	$^1D_2$?	− 3.2±3.3	+ 0.4±3.8	—	—	—
*$4s6q$	($l\geqq4$) ?	−32.0±3.4	−29.0±3.4	—	—	—
$4s9s$	$^1S_0$	− 5.1±2.2	− 4.2±2.0	—	—	—
$4s8d$	$^1D_2$	−14.3±2.9	− 6.4±2.0	− 1.3±5.5	—	+ 4.0±3.3
$4s7f$	$^1F_3$?	−18.7±2.4	− 9.9±2.2	—	—	—
*$4s7q$	($l\geqq4$) ?	−30.6±3.5	−25.5±3.5	—	—	—
$3d5s$	$^1D_2$	−11.2±3.8	− 4.9±3.8	—	—	—
$4s8f$	$^1F_3$?	−13.3±2.9	− 8.6±2.0	—	—	—
*$4s8q$	($l\geqq4$) ?	−20.9±4.3	−19.5±3.6	—	—	—
$4s9d$	$^1D_2$	− 6.1±2.3	− 4.7±2.5	—	—	—
$4s10d$	$^1D_2$	− 2.9±2.5	− 3.3±2.5	—	—	—
$4s11d$	$^1D_2$	− 3.1±2.8	− 3.3±2.6	—	—	—
$4s12d$	$^1D_2$	− 4.5±3.3	− 4.0±2.4	—	—	—
$4s13d$	$^1D_2$	− 8.5±3.3	− 5.2±2.6	—	—	—

* Quantum defcet is assumed to be 0. See § 3.2 in text.

of the shift are as follows. 1) In xenon, krypton and argon, red shifts are observed. They increase from argon through xenon. Exceptions are those for $-4p^2$, $-4s4f$, and $-4s7d$. 2) In helium and neon, blue shifts are observed. They are larger in helium than in neon. 3) The shift increases from *S-S* to *S-D* to *S-F* transitions with respect to any set of three adjacent *S*, *D*, and *F* upper levels in Table VI, with the same exceptions as 1). 4) The shift decreases with an increase in the principal quantum number n and reaches the minimum, with the same exceptions as 1) and 3).

3.4. The effective oscillator strength

The effective oscillator strength per unit rare-gas density

$$\frac{f_{\mathrm{CID}}}{[\mathrm{X}]} = \frac{mc}{\pi e^2}\int_{\mathrm{band}} \frac{k(\nu)L}{[\mathrm{X}][\mathrm{Ca}]L}\,\mathrm{d}\nu \qquad (2)$$

has been determined for the observed CID transitions. This would be directly given from the total absorption of eq.(1) in optically thin cases. However, the total absorption must be corrected for the opacity effect to obtain $K \equiv \int_{\mathrm{band}} k(\nu)L\mathrm{d}\nu$. The approximate method for this correction is described in ref. 11. In Fig. 3, the closed points give the resulting K values.

The relative precision or the "uncertainty" of the $K/[\mathrm{X}][\mathrm{Ca}]L$ value of each data point is estimated as follows. It is approximated to be $(e_{\mathrm{X}}^2+e_{\mathrm{H}}^2+e_{A}^2+e_{\mathrm{C}}^2)^{1/2}$, where e_{X} is the uncertainty of [X], within 1% in most cases apart from the systematic error, and 10 % in the worst case when $[\mathrm{Ca}]/[\mathrm{X}] \ll 1$ is not satisfied; e_{H} is the uncertainty of the measured total absorption, 1–25 % from the standard deviation of several measurements; e_{C} is the uncertainty of the opacity correction, which we estimate as 1/2 of the correction itself. On the basis of the uncertainty estimated above, the weighted average is done to give the $f_{\mathrm{CID}}/[\mathrm{X}]$ value. The resulting uncertainty is 2–3 % typically, and 10 % in the worst case.

The systematic errors are estimated as follows. An error owing to the procedure of the determination of [X] or of $[\mathrm{Ca}]L$ is $\simeq$10% in each case. The mixing of the absorption spectrum of a CID transition with an allowed-line wing or with an electric-quadrupole line or with another CID absorption gives rise to a systematic error. For $-4s8d\ ^1D_2$, for example, it is $\simeq$15 %.

The obtained $f_{\mathrm{CID}}/[\mathrm{X}]$ values are given in Table VII together with the estimated total uncertainty (including the estimates of the systematic errors). Most of the features of the shift summarized in the preceding section also hold for the present cases: $f_{\mathrm{CID}}/[\mathrm{X}]$ increases from argon to krypton to xenon, and is larger in

Table 7. $f_{CID}/[X]$ (10^{-26} cm^3) of the CID transitions from $4s^2\ ^1S_0$.

Upper levels		Xe	Kr	Ar	Ne	He
$4p^2$	$^1S_0$	445± 81	209± 52	41±9	43±11	116±29
$4s4f$	$^1F_3$	89± 26	56± 12	—	—	—
$4s5d$	$^1D_2$	110± 31	29± 8	—	8± 2	49± 9
$4s7s$	$^1S_0$	239± 63	64± 14	10±3	4± 1	27± 5
$4s5f$	$^1F_3$?	373±112	89± 20	8±3	—	—
$4s5g$	?	54±115	26± 6	—	—	—
$4s6d$	$^1D_2$	154± 60	56± 21	—	—	—
$4s8s$	$^1S_0$	51± 13	13± 4	—	—	—
$4s6f$	$^1F_3$?	362±109	94± 22	9±3	—	—
$4s7d$	$^1D_2$?	35± 15	21± 10	—	—	—
$4s6q$	($l\geqq4$) ?	31± 8	14± 5	—	—	—
$4s9s$	$^1S_0$	33± 10	—	—	—	—
$4s8d$	$^1D_2$	141± 49	28± 7	7±4	—	5± 2
$4s7f$	$^1F_3$?	195± 50	49± 12	—	—	—
$4s7q$	($l\geqq4$) ?	145± 41	54± 14	—	—	—
$3d5s$	$^1D_2$	60± 13	18± 5	—	—	—
$4s8f$	$^1F_3$?	207± 65	36± 10	—	—	—
$4s8q$	($l\geqq4$) ?	161± 44	53± 14	—	—	—
$4s9d$	$^1D_2$	31± 9	—	—	—	—
$4s10d$	$^1D_2$	29± 8	—	—	—	—
$4s11d$	$^1D_2$	29± 8	—	—	—	—
$4s12d$	$^1D_2$	31± 8	—	—	—	—

helium than in neon; $f_{CID}/[X]$ generally increases from *S-S* to *S-D* to *S-F*, and decreases with an increase in n.

4. Disucssion

According to the theory of the l-changing collision by Hickman,[15] the coupling between the two states concerned, which is caused by the interaction of the Rydberg electron with the rare-gas atom, is expressed in terms of the s-wave amplitude for low-energy-electron scattering from the rare-gas atom. Following this viewpoint, we compare the shifts and the effective oscillator strengths for the observed CID transitions with the s-wave amplitudes for the electron scattering.

For the s-wave amplitude, we use the functions given by O'Malley[24]

(Ne) $f_0(E)=-0.24-0.756\ E^{1/2}-0.031\ E\ \ln E+0.317\ E$,

(Ar) $f_0(E)=1.70-3.13\ E^{1/2}+0.92\ E\ \ln E+1.23\ E$,

(Kr) $f_0(E)=3.7-4.74\ E^{1/2}+3.01\ E\ \ln E+1.84\ E$,

(Xe) $f_0(E)=6.5-7.68\ E^{1/2}+8.58\ E\ \ln E+6.10\ E$,

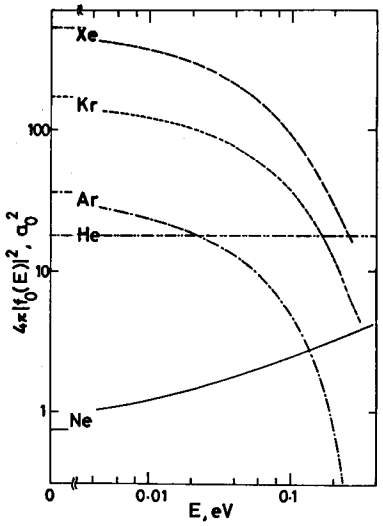

Fig. 4. s-wave amplitude for electron scattering by Xe, Kr, Ar, Ne, and He. The text discusses the correlation between the shift for the observed CID transition and the s-wave amplitude.

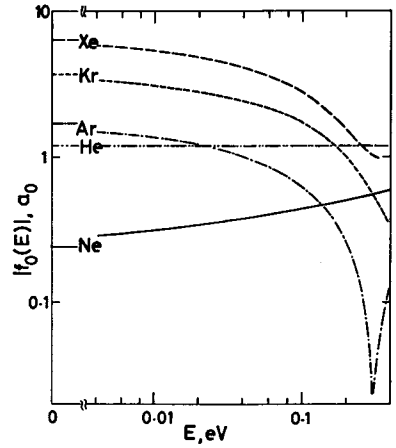

Fig. 5. The scattering cross section or $4\pi|f_0(E)|^2$ electron by Xe, Kr, Ar, Ne, and He. The text discusses the linear dependence of the $f_{CID}/[X]$ value on $4\pi|f_0|^2$.

where E is the energy of the electron in eV. For helium we approximate $f_0(E) = -1.19$.[24] Figures 4 and 5 show the s-wave amplitude $|f_0(E)|^2$ and the electron scattering cross section $4\pi|f_0(E)|$ of all rare gases as a function of E.

We find that the shifts of the observed CID transitions correlate with the s-wave amplitudes as follows. 1) The positive amplitudes which increase from argon through xenon correspond to the red shifts which increase in the same manner as the s-wave amplitudes. (See §3.3. 1.) 2) The negative amplitudes, the absolute values of which are larger for helium than for neon, correspond to the blue shifts larger for helium than for neon. (See §3.3. 2.) 3) The shifts for -4s5d and for -4s7s are proportional to the amplitudes at energies ~0.3 eV and ~0.15 eV, respectively.

As for effective ocsillator strengths, we find their linear dependence on $4\pi|f_0(E)|^2$: the oscillator strengths for -4s5d, -4s7s, and -4s8d are proportional to $4\pi|f_0|^2$ at ~0.2 eV, ~0.1 eV, and ~0.01 eV, respectively.

The fact that both the shift and the effective oscillator strength show a correlation with the s-wave amplitude for the electron scattering leads us to consider the process arising from the observed CID transitions as a low-energy-electron scattering by a rare-gas atom. This viewpoint is also supported by an approxi-

mate calculation. Using wavefunctions of the Bates-Damgaard type,[25] we made an approximate calculation for the adiabatic mixing of the atomic states due to the Fermi potential.[13] This calculation reproduced well the n-dependence of f_{CID}/[Xe] for $4s^2$-$4snd$ ($9 \leq n \leq 12$), as well as the dependence of f_{CID}/[X] for -$4s8d$ on rare-gas atoms, although the agreement of the absolute values was within a factor of 4.

In conclusion, we have established experimentally a close correlation between CID transitions and low-energy-electron-scattering parameters. It is considered that our observed correlation is well explained by the theory of the low-energy-electron scattering, and thorough theoretical treatments are now in progress.

References

1) M. Lapp: Phys. Lett. **23** (1966) 553.
2) J.A. Gwinn, P.A. Thomas and J.F. Kielkopf: J. Chem. Phys. **48** (1868) 568.
3) M. Dakhil and J.F. Kielkopf: J. Opt. Soc. Am. **67** (1977) 844.
4) A. Tam, G. Moe, W. Park and W. Happer: Phys. Rev. Lett. **35** (1975) 85.
5) G. Moe, A.C. Tam and W. Happer: Phys. Rev. **14** (1976) 349.
6) A. Gallagher and T. Holstein: Phys. Rev. **16** (1977) 2413.
7) J. Pascale: J. Chem. Phys. **67** (1977) 204.
8) B. Sayer, M. Ferray and J. Loizngot: J. Phys. B **12** (1979) 227.
9) B. Sayer, M. Ferray, J.P. Visticot and J. Lozingot: J. Phys. B **13** (1980) 177.
10) T. Fujimoto, K. Ueda and K. Fukuda: J. Quant. Spectrosc. Radiat. Transfer **21** (1979) 89.
11) K. Ueda, T. Fujimoto and K. Fukuda: to be published in J. Phys. Soc. Jpn.
12) K. Ueda, Y. Ashizawa, T. Fujimoto and K. Fukuda: J. Phys. Soc. Jpn. **48** (1980) 345.
13) E. Fermi: Nuovo Cimento **11** (1934) 157.
14) E. Amaldi and E. Segre: Nuovo Cimento **11** (1934) 145.
15) A.P. Hickman: Phys. Rev. A **19** (1979) 994.
16) M. Matsuzawa: J. Phys. B **12** (1979) 3743.
17) T.F. Gallagher, S.A. Edelstein and R.M. Hill: Phys. Rev. Lett. **35** (1975) 644.
18) T.F. Gallather, S.A. Edelstein and R.M. Hill: Phys. Rev. A **15** (1977) 1945.
19) T.F. Gallagher, W.E. Cooke and S.A. Edelstein: Phys. Rev. A **17** (1978) 904.
20) M. Hugon, F. Gounand, P.R. Fournier and J. Berlande: J: Phys. B **12** (1979) 2707.
21) W.H. Smith and H.S. Liszt: J. Opt Soc. Am. **61** (1971) 938.
22) G. Risberg: Ark. Fys. **37** (1968) 231.
23) J.A. Armstrong, P. Esherick and J.J. Wynne: Phys. Rev. A **15** (1977) 180.
24) T.F. O'Malley: Phys. Rev. **130** (1963) 1020.
25) D.R. Bates and A. Damgaard: Philos. Trans. R. Soc. London A **242** (1949) 101.